# Planning Time for Peripheral Blood Stem Cell Infusion After High-Dose Targeted Radionuclide Therapy Using Dosimetry

Sui Shen, PhD[1]; Sally J. DeNardo, MD[2]; Carol M. Richman, MD[2]; Aina Yuan, PhD[2]; Christine Hartmann Siantar, PhD[3]; Robert T. O'Donnell, MD, PhD[2,4]; Linda A. Kroger, MS[2]; and Gerald L. DeNardo, MD[2]

*[1]Department of Radiation Oncology, University of Alabama, Birmingham, Alabama; [2]Department of Internal Medicine, Hematology/Oncology Division, University of California Davis, Sacramento, California; [3]Lawrence Livermore National Laboratory, Livermore, California; and [4]Veteran's Administration Northern California Healthcare System, Mather, California*

Myelotoxicity can be ameliorated by peripheral blood stem cell (PBSC) infusion. Continuous irradiation by radioactivity retained in the body after high-dose radioimmunotherapy can damage PBSCs if they are transfused too early. Previously, infusion time was predetermined using the radioactivity concentration in the blood. This study proposes to plan PBSC infusion time based on noninvasive dosimetry that considers damage of PBSCs during PBSC circulation and residence in organs with high radioactivity. **Methods:** The method considers a time-varying distribution of PBSCs and radioactivity in tissues. Five breast cancer patients received $^{111}$In-2IT-BAD-m170 for imaging, and 3 of the 5 received high doses of $^{90}$Y-2IT-BAD-m170 therapy followed by PBSC infusion. $^{90}$Y concentrations in tissues were extrapolated from quantitative imaging of $^{111}$In, and $^{90}$Y blood concentrations were determined from $^{90}$Y in serial blood samples. The radiation dose to PBSCs was determined by time integration of the organ dose rate and PBSC distribution rate. The radiosensitivity of PBSCs was determined by measuring survival of granulocyte-macrophage colony-forming units with $^{90}$Y in cell culture. **Results:** The mean effective half-life of $^{90}$Y within the imaging period (up to 6 d) was 3.7 d for liver, 2.4 d for spleen, 2.1 d for kidneys, 1.8 d for lungs, and 1.6 d for blood. The survival fractions of PBSCs in patients were determined as functions of the infusion time and the injected dose of $^{90}$Y-2IT-BAD-m170. To achieve 90% PBSC survival rate for a 2.0-GBq injection dose, PBSC dosimetry suggested a time interval of 13 d after radioimmunotherapy for PBSC infusion. In contrast, the simple blood concentration method suggested an interval about 7 d for the same PBSC survival rate. In our clinical practice, an interval of 2 wk has been used and worked well. **Conclusion:** A noninvasive dosimetry method was developed for optimizing the time interval for PBSC infusion after high-dose radionuclide therapy. Our studies suggested that the PBSC dosimetry method was more effective than the blood concentration method in determining the optimal time to reinfuse PBSCs for radiopharmaceuticals that have much a higher activity concentration in organs than that in the blood.

Received Dec. 16, 2004; revision accepted Feb. 26, 2004.

For correspondence or reprints contact: Sui Shen, PhD, Department of Radiation Oncology, University of Alabama at Birmingham, 1824 6th Ave. S., Wallace Tumor Institute, Room 124, Birmingham, AL 35294.

E-mail: sshen@uabmc.edu

**Key Words:** treatment planning; peripheral blood stem cell; bone marrow; radiation dosimetry; radioimmunotherapy

**J Nucl Med 2005; 46:1034–1041**

Targeted radionuclide therapy, including radioimmunotherapy, is an innovative approach that systemically delivers localized radiation using target molecules directed to cancer cells. Encouraging results have been obtained in radioimmunotherapy for lymphoma (*1–4*). However, the efficacy of radiolabeled antibodies for solid tumors such as breast cancer has been limited by several factors, including (a) slow accumulation of antibodies at tumor sites, (b) relatively slow clearance of antibodies from the blood, and (c) relative radioresistance of solid tumors compared with lymphoma. Consequently, whereas tumors often receive insufficient radiation for a significant response, radiation dose to the radiosensitive normal organ, marrow, can readily reach the tolerable limit. Myelosuppresion can be ameliorated with autologous bone marrow transplantation or peripheral blood stem cell (PBSC) infusion, as illustrated first by Press et al. in treatment of lymphoma (*2*) and followed by others in treatment of breast cancer (*5–9*), colon cancer (*10*), and lymphoma (*11*). These studies suggested that a higher tumor response rate was associated with a higher radioactive injection dose followed by bone marrow reconstitution.

In treatments having PBSC support, the time interval between the radioactive dose injection and PBSC infusion is an important parameter for optimal patient management. Although PBSCs can be injured by continuous irradiation from exposure to irradiation from radioimmunotherapy if they are transfused too early, patients can also develop serious complications from low levels of neutrophils or platelets if PBSCs are transfused too late. Previously, the time interval for PBSC infusion was determined by a calculation method based on blood radioactive concentration (*5*). The blood activity concentration threshold was deter-

mined from an in vitro study in which rates of PBSC survival were measured at various radioactivity concentrations. However, our initial clinical results on hematopoietic reconstitution after $^{90}$Y radioimmunotherapy were unsatisfactory when the PBSC infusion time was determined by $^{90}$Y concentrations in the blood. Recovery of blood counts was delayed even when $^{90}$Y concentration in the blood was well below the activity concentration threshold determined in vitro.

Radioactivity concentration in the liver, spleen, and kidneys can be much higher than that in the blood, so that PBSCs can be damaged during their circulation through these organs. PBSCs can be further damaged after homing (a process in which PBSCs migrate form peripheral blood to bone marrow) if marrow or bone has radioactive uptake. Therefore, the radiation dose from radioactivity in the blood is only one part of the total radiation dose to PBSCs. To address the issues described here, we propose a new, noninvasive method for planning PBSC infusion time based on imaging and radiation dosimetry. The proposed method considers (a) time-varying radiation dose rate to PBSCs from radioactivity in the blood and other source organs, (b) time-varying PBSC distribution in the body during the homing, and (c) radiation dose to PBSCs from radioactivity in bone and marrow after PBSC homing.

## MATERIALS AND METHODS

### Radiopharmaceuticals

Monoclonal antibody 170H.82 (m170) is a murine monoclonal IgG1 antibody that is reactive with the synthetic Thomsen–Friedenreich antigen family. It was obtained from Biomira. m170 was 95% monomeric IgG by polyacrylamide gel electrophoresis and met U.S. Food and Drug Administration guidelines for administration to patients. m170 binds to a variety of human adenocarcinomas, including breast cancer (*12,13*). m170 was radiolabeled with $^{90}$Y or $^{111}$In via DOTA-2IT-BAD (2-iminothiolane-2-[*p*-(bromoacetamido)benzyl]-1,4,7,10-tetraazacylododecane-*N,N′-N″N‴*-tetraacetic acid).

### Patients

Five patients with previously treated metastatic breast cancer were enrolled in this study. These patients had failed at least one combined chemotherapy regimen and had measurable tumors that were reactive to m170 by immunoperoxidase staining. All patients who participated in the study signed written informed consents for the protocol that was approved by the University of California, Davis, Institutional Review Board for studies involving human subjects and the Radiation Use Committees, under a physician-sponsored Investigational New Drug authorization from the U.S. Food and Drug Administration (FDA). As required by the FDA, treatment was initiated until imaging studies were completed for the first 3 patients. Therefore, 2 of first 3 patients were not treated. All patients received $^{111}$In-2IT-BAD-m170 for imaging and 3 received high-dose $^{90}$Y-2IT-BAD-m170 followed by PBSC infusion. The protocol planned for 3-cycle fractionated treatments; only 1 fraction was given to each of 3 patients (2.0, 2.3, and 1.4 GBq) due to progressive disease, human anti–monoclonal antibody (HAMA), and patient decision due to lack of an objective response (disease was stable) (*13*). All patients had normal complete blood counts before $^{90}$Y-2IT-BAD-m170 therapy and had Karnofsky performance scores of ≥70%. Patients were 41–50 y old.

### PBSC Mobilization and Collection

Patients received granulocyte colony-stimulating factor at 10 μg/kg/d subcutaneously. On the fifth day, PBSCs were harvested by apheresis as described previously (*5,7*). The goal was to collect a total of $6 \times 10^5$ granulocyte–macrophage colony-forming units (GM-CFUs) and $6 \times 10^6$ CD34+ cells per kilogram of patient weight to support the 3 planned therapy cycles. PBSCs were harvested using a Cobe Spectra system (Cobe BCT). Aliquots of at least 1 apheresis per patient were evaluated for tumor cells by a sensitive immunoperoxidase assay that can detect approximately 1 tumor cell in 1 million cells (BIS Laboratories). Cells were cryopreserved and stored in liquid nitrogen. At least $2 \times 10^6$ CD34+ cells per kilogram were transfused to patients after $^{90}$Y-2IT-BAD-m170 therapy.

### PBSC Survival with $^{90}$Y In Vitro Cell Cultures

The effect of $^{90}$Y concentration on PBSC survival rate was evaluated by sequential counting of GM-CFUs from PBSCs in vitro. Whereas GM-CFUs represent committed progenitor cells and not primitive multipotential precursors, this cell population contributes predominantly to early engraftment. Five cell cultures were prepared with culture trays having $^{90}$Y concentration levels of 0.0, 0.37, 3.7, 37, and 370 kBq/mL. Each culture tray had 4 wells with identical $^{90}$Y concentration. All 20 wells (in 5 trays) were inoculated with the same initial number of cells from a PBSC collection. The volume of $^{90}$Y solution in each well (5-mm height, 16-mm diameter) was 0.5 mL. The trays were placed in an incubator at 37°C with 100% humidity for 15 d to allow for colony formation. The number of GM-CFUs was counted using an inverted microscope as described previously (*7*).

The $^{90}$Y radiation dose to the PBSCs in the well was determined by:

$$D_{PBSC} = \int_0^{15d} A \cdot \phi \cdot \Delta_{^{90}Y} \cdot \exp(-0.693 \cdot t/2.67)dt, \quad \text{Eq. 1}$$

where A is $^{90}$Y concentration (kBq/mL) in the well, $\phi$ is the fraction of $^{90}$Y energy absorbed in PBSCs from 0.5-mL $^{90}$Y solution in the well, $\Delta_{^{90}Y}$ is the total mean $^{90}$Y energy emitted per nuclear transition (1.50E−13 Gy kg/Bq s), and 2.67 d (64 h) is the physical half-life of $^{90}$Y. Based on numeric integration of all voxels (0.001 mm$^3$) using $^{90}$Y percentile data (*14*), an absorbed fraction of 0.49 was determined for the radiation dose from $^{90}$Y uniformly distributed in 0.5-mL solution to PBSCs settled in a methyl cellulose layer at the bottom of the well about 0.2-mm thick. The PBSC survival was described by a linear-quadratic formula (*15*):

$$\ln\left(\frac{N_{15d}}{N_0}\right) = -\alpha \cdot D_{PBSC} + \frac{0.693 \cdot 15d}{T_{pot}}, \quad \text{Eq. 2}$$

where $N_{15d}$ is the number of cells surviving after 15-d irradiation, $N_0$ is the initial number of cells, $\alpha$ is the coefficient of nonrepairable damage per gray, and $T_{pot}$ is the doubling time for PBSC proliferation. The coefficient of repairable damage, $\beta$, is assumed to be zero as bone marrow stem cells do not exhibit a late radiation effect (*16*). As the initial cell numbers were identical in the control and irradiated wells, Equation 2 can be simplified as:

$$\ln\left(\frac{N_{15d}}{N_{control}}\right) = -\alpha \cdot D_{PBSC}, \qquad \text{Eq. 3}$$

where $N_{control}$ is the number of cells in the control well in which $^{90}Y$ activity was zero.

### Dosimetry Data Collection and Analysis

Imaging and blood data collection and analysis have been described in detail previously (*13,17,18*). Briefly, planar conjugate views were acquired with a Bodyscan dual-detector camera (Siemens Medical Systems, Inc.). Medium-energy collimators were used with energy windows centered at 171 and 245 keV with 15% width for $^{111}In$. Whole-body scans and static images of the skull, chest, abdomen, and pelvis were acquired immediately and at approximately 4, 24, 48, 72, and 144 h.

Liver, spleen, lungs, kidneys, and lumbar vertebrae (L2–L4) were visualized above body background tissue and their uptake of $^{111}In$-2IT-BAD-m170 was quantified. The operator reviewed CT images to facilitate region-of-interest (ROI) determination. ROIs for the whole body and the organs were manually defined based on visual boundary. The geometric-mean quantification was used for liver and lungs. The attenuation correction factor for liver and lung was determined using transmission scan images obtained with a rod source containing about 93 MBq $^{111}In$. The effective-point-source quantification was used for spleen, kidneys, and lumbar vertebrae L2–L4 for marrow (*19–21*). Photon attenuation was corrected using measured $\mu$ values that matched the small source geometry. A 10-mL calibrated source of 7.4 MBq $^{111}In$ was used to convert ROI counts to megabecquerels of $^{111}In$ and $^{90}Y$, assuming identical distributions in all organs except for bone marrow. Cumulated $^{90}Y$ activity and effective clearance half-life ($T_{eff}$) were determined by fitting the organ activity data to a monoexponential curve. Liver, spleen, kidney, and lung radiation doses from $^{90}Y$ were calculated using S values from MIRDOSE3 software (*22*). S values for source and target in red marrow and bone endosteum were obtained from a revised model based on the Eckerman and Stabin model and the Bouchet and Bolch model for high-energy $\beta$-particles of $^{90}Y$ (*23–25*).

Serial blood samples were collected after dose injection of $^{90}Y$-2IT-BAD-m170 at approximately 0.083, 0.5, 1, 2, 4, 24, 48, 48, 72, and 144 h. An aliquot (1 mL) of each sample was counted in a $\gamma$-well counter calibrated for $^{90}Y$ to determine $^{90}Y$ concentration (kBq/mL) in the blood. The cumulated activity was determined by fitting data to a biexponential curve with $\alpha$- and $\beta$-clearance phases. Time-dependent radiation dose to PBSCs from blood was predominated by the $\beta$-clearance phase at the time of PBSC infusion.

### PBSC Dosimetry

After intravenous infusion of PBSCs, stem cells circulate in the blood through various organs before they migrate into the cellular compartment of the marrow. Thus, radiation doses to PBSCs from $^{90}Y$ in major organs need to be considered (Fig. 1). The radiation dose to PBSCs in the organ, $D_{PBSC \leftarrow organ}$, can be described as a function of time for PBSC infusion $T_{infu}$ ($T_{infu} = 0$ at $^{90}Y$ injection):

$$D_{PBSC \leftarrow organ}(T_{infu}) = R_{organ_i}(T_{infu}) \cdot \int_0^{\infty} \exp(-0.693 \cdot t/T_{eff}) \cdot PBSC_{organ}(t)dt, \qquad \text{Eq. 4}$$

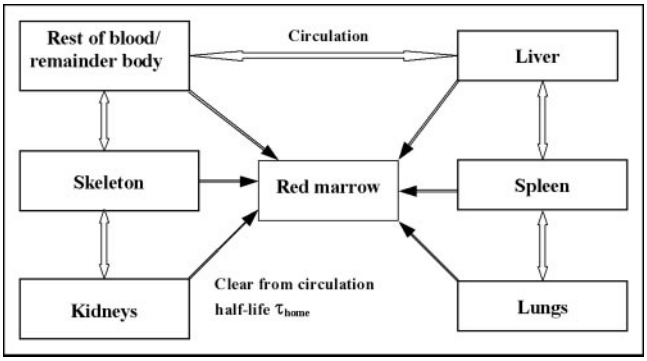


**FIGURE 1.** Schematic diagram to illustrate circulation of PBSCs in major organs and migration of PBSCs to marrow with a half-life of $\tau_{home}$ cleared from blood.

where $R_{organ}(T_{infu})$ is the organ dose rate at the time of PBSC infusion, $T_{eff}$ is the organ effective clearance half-life, and $PBSC_{organ}(t)$ is the fraction of PBSCs in the organ at time t after PBSC infusion (t = 0 at PBSC infusion). The cumulated dose was integrated from the time of PBSC infusion.

For a $\tau_{home}$ half-life for PBSCs cleared from circulation, the PBSC distribution in the organ, except for red marrow, can be described as function of time:

$$PBSC_{organ}(t) = F_{organ} \cdot \exp(-0.693 \cdot t/\tau_{home}), \qquad \text{Eq. 5}$$

where $F_{organ}$ is the fraction of total blood volume in the organ. The blood volume in the liver, spleen, lungs, kidneys, bone, and marrow can be found in the literature for the Reference Man (Table 1) (*26*). The volume of the remainder of the blood was determined by subtracting blood volume in the liver, spleen, kidneys, lungs, marrow, and bone from the total blood volume. The $\tau_{home}$ was estimated to be 55 h based on a reported measurement that 20% of stem cells migrate to the murine marrow 18 h after stem cell infusion (*27*).

The amount of PBSCs that accumulate in the red marrow can be determined by:

$$PBSC_{red\ marrow}(t) = F_{red\ marrow} + (1 - F_{red\ marrow}) \cdot (1 - \exp(-0.693 \cdot t/\tau_{home})) = 1 - (1 - F_{red\ marrow}) \cdot \exp(-0.693 \cdot t/\tau_{home}). \qquad \text{Eq. 6}$$

## RESULTS

### PBSC Survival in $^{90}Y$-Treated Cell Culture

The GM-CFU survival fraction as a function of $^{90}Y$ concentration is shown in Figure 2. The natural logarithms of survival fraction data were least-square fitted to the activity concentration up to 37 kBq/mL. Data for 370 kBq/mL concentration could not be included in data fitting because there were no GM-CFUs found at a concentration level of 370 kBq/mL and, mathematically, ln(0) is uncertain ($-\infty$). Only part of the $^{90}Y$ energy was deposited to PBSCs. Based on numeric integration, 0.5 mL of 37 kBq/mL $^{90}Y$ solution delivers a mean dose of 0.88 Gy in 15 d to PBSCs in a methylcellulose layer at the bottom of the well. The fitted value for the coefficient of nonrepairable damage ($\alpha_{PBSC}$) was 0.744 $Gy^{-1}$ when the survival rate was ex-

**TABLE 1**
Organ Mass and Fraction of Total Blood Volume in Organ of Reference Man

| Organ | Mass (g) | Fraction of total blood volume (%) |
|---|---|---|
| Liver | 1,800 | 10.0 |
| Spleen | 150 | 1.4 |
| Lungs | 1,200 | 12.5 |
| Kidneys | 310 | 2.0 |
| Skeleton | 10,500 | 7.0 |
| Bone | 5,500 | |
| Cortical bone | 4,400 | 1.2 |
| Trabecular bone | 1,100 | 0.8 |
| Red marrow | 1,170 | 4.0 |
| Remainder of body | 59,040 | 67.1 |
| Remainder of blood | | 67.1 |
| Total blood | | 100 |

Data are from (*26*).

**TABLE 2**
Mean $T_{eff}$ and $^{90}Y$ Radiation Dose for 5 Patients Receiving $^{111}In$-2IT-BAD-m170

| Tissue | $T_{eff}$ (h) | Dose (mGy/MBq) |
|---|---|---|
| Liver | NA | 4.8 |
| Spleen | 58 | 2.8 |
| Kidneys | 50 | 1.9 |
| Lungs | 43 | 1.7 |
| Marrow (imaging L2–L4) | 60 | 1.6 |
| Body | 55 | 0.61 |
| Blood | 38 | 7.1* |

*This is accumulated activity concentration (7.1 kBq h/MBq/g) in blood as actual blood dose is complicated by various blood vessel sizes.

NA = not available as uptake in liver typically increased during 6-d imaging period.

pressed as exp($-\alpha$D) or 0.664 $Gy^{-1}$ if the survival rate was expressed as exp($-0.064 - \alpha$D).

### PBSC Dosimetry for Individual Patients: Example of Calculation

The mean $T_{eff}$ and radiation dose for $^{90}Y$-2IT-BAD-m170 were determined for liver, spleen, kidneys, lungs, marrow (by imaging L2–L4), blood, and body in 5 patients (Table 2). To illustrate the process for planning infusion time, the detailed calculation for 1 patient was as follows:

After completing 6 d of an $^{111}In$-2IT-BAD-m170 imaging study, 1 patient received 2.0 GBq of $^{90}Y$-2IT-BAD-m170. Seven days (168 h) after injection of the dose, the $^{90}Y$ concentration in the blood was 7.4 kBq/mL. The effective β-clearance half-life was 31 h. What is the radiation dose to PBSCs if PBSCs are transfused at 168 h after injection?

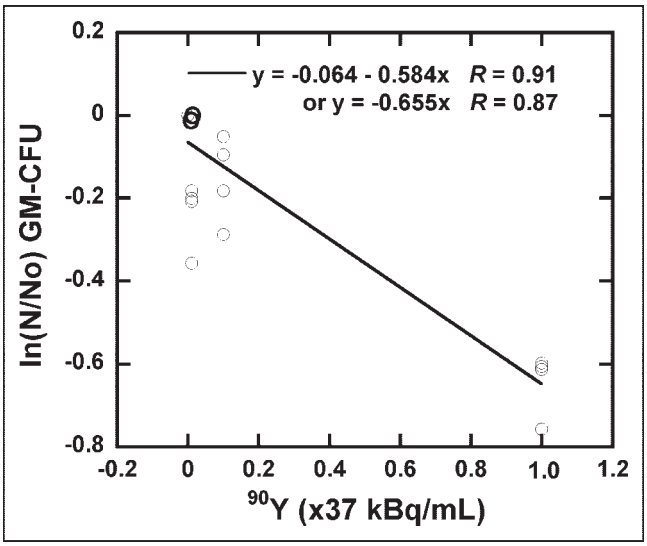


**FIGURE 2.** Effect of $^{90}Y$ concentration on survival of GM-CFUs from stem cells in cell cultures.

When should PBSCs be transfused if killing of PBSCs is to be kept <10%?

*Organ Effective $T_{eff}$, Uptake, and Concentration of $^{90}Y$ at 168 Hours After Injection.* The $T_{eff}$ for the liver could not be determined by monoexponential curve fitting, as the liver uptake was increased from 10 %ID (percentage injected dose) immediately after injection to 20 %ID 144 h after injection (last imaging time point). An effective half-life of 64 h (physical half-life of $^{90}Y$) was assumed after 144 h in the liver, assuming a constant biologic uptake after the last imaging time point (Table 3). The effective half-life of the remainder of the body was derived from the effective half-life of liver, spleen, kidneys, lungs, marrow, bone, and total body.

An $^{90}Y$ concentration of 5.2 kBq/g in bone (Table 3) was estimated on the basis of the reported difference in $^{111}In$ and $^{90}Y$ concentration in bone or marrow biopsy (*28*) adjusted for the difference in chelation (*29*). The amount of $^{90}Y$ in cortical bone and trabecular bone was determined on the basis of the reported ratio of trabecular-to-cortical bone surface area (10.5:6.5) (*26*).

The radiation dose in the remainder of the blood was considered to be 2 parts: (a) 100% absorption of $^{90}Y$ energy for 1.4 kBq/g in the blood as the $^{90}Y$ concentration in the remainder of the body without blood was 1.4 kBq/g (Table 3); and (b) for the remaining 3.5 kBq/g of $^{90}Y$ in the blood, an absorption fraction value of 0.54 was determined using reported $^{90}Y$ absorption fractions for various blood vessels in the arterial and venous systems (*30*), excluding the pulmonary system.

*Organ Dose Rate at 168 Hours After Dose Injection: Dose to PBSCs.* Except for bone and red marrow, the organ dose rate was contributed from $^{90}Y$ located in the organ itself. At 168 h after dose injection, the dose rate to marrow was 0.49 cGy/h from $^{90}Y$ in marrow and 0.20 cGy/h from $^{90}Y$ in bone. The dose rate to bone was 0.27 cGy/h from $^{90}Y$ in bone and 0.31 cGy/h from $^{90}Y$ in marrow. In the total

**TABLE 3**
Dosimetry Data for 1 Patient Given 2.00 GBq of $^{90}$Y-2IT-BAD-m170

| Organ | $T_{eff}$ (h) | Uptake at 168 h (MBq) | Concentration at 168 h (kBq/g) | Organ dose rate at 168 h (cGy/h) | PBSC dose (cGy) |
|---|---|---|---|---|---|
| Liver | 64 | 65 | 36 | 1.9 | 8.3 |
| Spleen | 58 | 4.0 | 27 | 1.4 | 0.82 |
| Kidneys | 60 | 5.4 | 18 | 0.94 | 0.78 |
| Lungs | 42 | 6.1 | 5.1 | 0.27 | 1.2 |
| Red marrow | 55 | 24 | 21 | 0.69 | 29 |
| Bone | 64 | 29 | 5.2 | 0.58 | 0.48 |
| Cortical bone | 64 | 11 | 2.5 | | |
| Trabecular bone | 64 | 18 | 16 | | |
| Total blood | 31 | 27 | 4.9 | | |
| Remainder of blood | 31 | 19 | 4.9 | 0.25 | 4.9 |
| Total body | 55 | 240 | 0.0033 | | |
| Remainder of body | 46 | 100 | 0.0016 | | |
| Remainder of body, no blood | 49 | 83 | 1.4 | | |

To illustrate the computing process, uptake in cortical bone, trabecular bone, total blood, total body, remainder of body, and remainder of body without blood was listed but was not needed for organ dose rate and PBSC dose.

radiation dose to PBSCs, 65% of the dose was contributed from $^{90}$Y in the marrow and bone, 12% was contributed from $^{90}$Y in the remainder of the blood, and 11% was contributed from $^{90}$Y in the liver (Table 3).

Similarly, using the same computing procedures, the radiation dose to PBSCs would be 50.4 cGy (12.4 cGy from liver, 31.2 cGy from marrow, 4.5 cGy from remainder of the blood or body) for patient 2 receiving 2.1 GBq $^{90}$Y if PBSCs were infused 7 d after $^{90}$Y injection. The radiation dose to PBSCs would be 32.2 cGy (8.5 cGy from liver, 15.9 cGy from marrow, 6.2 cGy from remainder of the blood or body) for patient 3 receiving 1.4 GBq $^{90}$Y if PBSCs were infused 7 d after $^{90}$Y injection.

*PBSC Survival and Infusion Time.* The PBSC survival rate was determined as $e^{-0.744D}$ as described. For a given injection dose, the PBSC survival could be determined as a function of PBSC infusion time (Fig. 3). For treatment planning before dose injection, physicians can review patient-specific isosurvival curves as a function of injection dose and the time interval for PBSC infusion (Fig. 4). For example, for the 2.0-GBq dose injection to this illustrated patient, 80% PBSC survival requires a time interval at least 9 d, and 90% survival requires a time interval at least 13 d (Fig. 4). In our clinical practice, an interval of 2 wk has been used. This infusion time interval worked well, as all 3 patients demonstrated evidence of hematologic recovery.

## DISCUSSION

Radiation-induced myelotoxicity is often dose limiting in radionuclide therapy that does not include bone marrow reconstitution. For treatment without marrow reconstitution, the challenges in marrow dosimetry have been discussed extensively in the literature (*20,23,31–37*). However, in high-dose treatment with marrow reconstitution, there has been no detailed analysis of radiation damage to PBSCs during circulation and after homing that can cause a delayed blood count recovery.

After PBSC infusion, several critical events determine the final engraftment results. These events include the time that PBSCs freely circulate in blood vessels, time that PBSCs traverse the endothelial barrier, time that PBSCs migrate into tissue spaces, and, finally, residence in one particular tissue space. In each of these events, PBSCs can be damaged by irradiation from radioactivity located in the tissues. In the current study, we proposed a noninvasive method to calculate radiation dose to PBSCs that accounts for time-varying distributions of PBSCs and radioactivity in tissues.

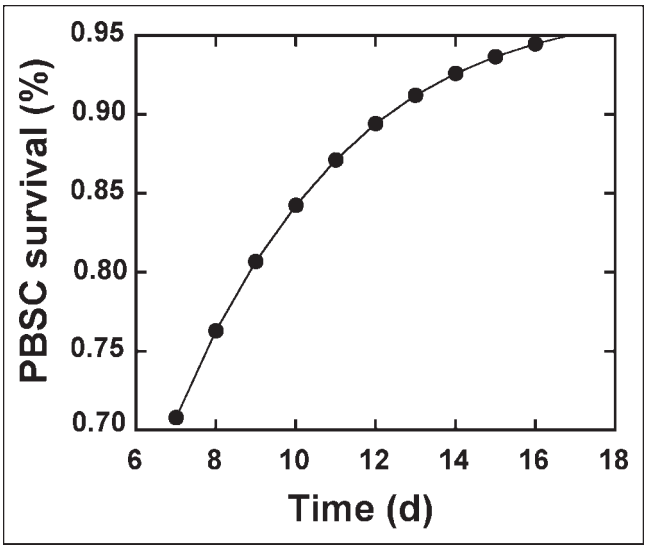


**FIGURE 3.** Calculated PBSC survival as function of infusion time for patient receiving 2.0 GBq $^{90}$Y-2IT-BAD-m170, given patient-specific tissue effective half-lives and radiation doses (Table 3).

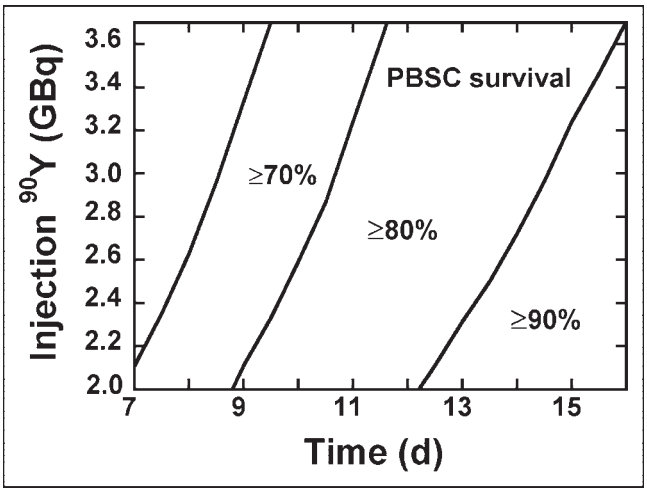


**FIGURE 4.** Isosurvival curves for planning time for PBSC infusion. Isosurvival curves of 70%, 80%, and 90% were determined as function of injection dose and infusion time.

Initially, we estimated the time interval for PBSC infusion based on the $^{131}$I concentration level in the blood in breast cancer patients treated using $^{131}$I-labeled chimeric L6 antibody (*5*). In limited observations of patients receiving high-dose $^{131}$I-labeled chimeric L6, the PBSC infusion time based on the $^{131}$I concentration in the blood worked reasonably well. However, in patients receiving high-dose $^{90}$Y-2IT-BAD-m170, the results were unsatisfactory when the time for PBSC infusion was based on the $^{90}$Y concentration in the blood. Recoveries of blood counts were unexpectedly delayed in 1 transfused patient when the blood level of radioactivity was below the threshold determined in vitro. This prompted further analysis of other possible contributions to the irradiation of the infused PBSCs. In the current analysis, it is quite clear that the dose from $^{90}$Y in the blood accounts for only a portion of the total dose to PBSCs. Although the remainder of the blood has 74% blood volume (Table 1), it contributes 12% of the total dose to PBSCs (Table 3).

In our illustrated case, the majority of the radiation dose to PBSCs was from $^{90}$Y in marrow and bone as PBSCs accumulate in marrow over time. In treatment with $^{90}$Y-labeled targeted molecules, the radiation dose to PBSCs in the marrow is contributed from $^{90}$Y in the blood and $^{90}$Y in the bone if there is no active uptake of target molecules by the marrow. The DOTA chelator used in this study has been shown to hold $^{90}$Y and $^{111}$In stably (*29,38*). Although minimal $^{90}$Y and $^{111}$In can escape from the chelator, lumbar vertebrae were still visible in $^{111}$In-2IT-BAD-m170 images. It is quite common to visualize lumbar vertebrae in $^{111}$In-labeled antibody images of patients without known marrow malignancy (*21,39*), although $^{111}$In or $^{90}$Y is still held by the chelator.

Therefore, in the current proposed method, we estimated $^{111}$In uptake in the marrow using the imaging method to include $^{111}$In that was distributed in the blood and in the marrow. The difference between the $^{111}$In amount in marrow and the $^{90}$Y amount in bone was considered using data reported for patient core biopsies that showed that the mean difference between $^{90}$Y and $^{111}$In concentration in bone and marrow was 0.003 %ID/g with MX-diethylenetriaminepentaacetic acid (methylbenzyl-DTPA [MX-DTPA]) chelator (*28*). To adjust the difference between the MX-DTPA chelator and the DOTA chelator, a value of 0.0016 %ID/g was estimated based on reported autoradiographic measurements in mice that the mean $^{90}$Y uptake in bone with MX-DTPA chelator was 1.88 times higher than that with the DOTA chelator (*29*). This 0.0016 %ID/g corresponds to 5.2 kBq/g in bone at 168 h after injection in our calculation example (Table 3). Image quantification in the lumbar vertebrae region (*19,20*) assumes that the regional activity concentration in vertebrae can represent the mean activity concentration in total marrow. This assumption could be problematic if patients have marrow involved with cancer. In the current patient population, there was no hot spot in or near the L2–L4 lumbar vertebrae ROI. Nevertheless, if there are hot spots in the skeletal region, selection of the ROI for these particular patients should be carefully evaluated on a case-by-case basis.

The $^{90}$Y concentration in bone and marrow can be directly determined from bone marrow biopsy. Wong et al. used bone marrow biopsy to estimate the $^{90}$Y radiation dose to autologous stem cells (*9*). Initially, they transfused 25% of the stem cells at 5 d after $^{90}$Y injection (0.56 GBq/m$^2$) regardless of the variation in $^{90}$Y distribution among the patients. The remaining 75% of the stem cells were transfused at the time point at which the estimated remaining marrow dose was ≤5 cGy, as determined by patient-specific bone marrow biopsy. Their protocol was modified for a dose level of 0.83 GBq/m$^2$, at which 25% of the stem cells were transfused when the remaining marrow dose was ≤5 cGy, and the remaining 75% were transfused when the absolute granulocyte count was <1,000/μL. Their transfusion schedules worked well as all patients demonstrated evidence of hematologic recovery. According to the current analysis, the sum of radiation doses from liver, spleen, kidneys, lungs, and the remainder of the blood was about half of the dose from marrow and bone (Table 3), and 5 cGy to PBSCs would damage only 3.7% of the total PBSCs. Therefore, dose contribution from other major organs and blood may be ignored if a low threshold value for marrow dose is selected deliberately. Although bone marrow biopsy provides a direct, patient-specific, measurement of radioactivity, its accuracy often suffers from large variations dependent on sampling. The current imaging method is noninvasive and is not limited by the potential sampling error.

Regeneration of the hematopoietic system is complex. There are many factors other than radiation dose that may affect the final engraftment results, including the number and "quality" of stem cells harvested, particularly in heavily pretreated patients, or production of inhibitory cytokines—

for example, in association with infection that interferes with hematopoietic cell proliferation. These factors are beyond the scope of a method that is based on "a typical" patient. The current proposed method considers the radiation damage to PBSCs from all sources and provides a practical method to determine the infusion time under a typical patient condition. The success of engraftment is dependent on the short-term (~4 wk) repopulating cells to provide transient protection, and irradiation from radionuclide therapy is typically during this short term; therefore, radiation damage to PBSCs should be kept insignificant. It seems that a 90% PBSC survival rate is appropriate to determine infusion time. This corresponds to an infusion time interval of ~2 wk in our patients receiving 1.4–2.1 GBq $^{90}$Y-2IT-BAD-m170 and it worked well, as all 3 patients demonstrated evidence of hematologic recovery. The calculation of radiation dose to PBSCs can be easily implemented using spreadsheet software, such as Excel (Microsoft). Once the spreadsheet program has been established, the PBSC dose and survival rate can be calculated instantly by simply entering patient-specific tissue effective half-lives and radiation doses into the spreadsheet.

## CONCLUSION

PBSC infusion is a critical component of many high-dose targeted radionuclide therapies. A noninvasive dosimetry method was developed for planning the time for PBSC infusion after high-dose radioimmunotherapy. The method calculates the radiation dose to PBSCs from radioactivity in all sources with time-varying distributions of PBSCs and radioactivity. Our studies suggested that the PBSC dosimetry method was more effective than the blood concentration method in predicting the best time to reinfuse PBSCs for radiopharmaceuticals that have a much higher activity concentration in organs than that in the blood.

## ACKNOWLEDGMENTS

This work was supported by grant CA 47829 from the U.S. Public Heath Service, National Cancer Institute. The authors thank Tina Schuermann for technical assistance in the GM-CFU survival experiment with $^{90}$Y. Part of this work was presented at the 49th Annual Meeting of the Society of Nuclear Medicine, Los Angeles, CA, June 15–19, 2002 (*40*).

## REFERENCES

1. DeNardo SJ, DeNardo GL, O'Grady LF, et al. Treatment of B cell malignancies with $^{131}$I Lym-1 monoclonal antibodies. *Int J Cancer.* 1988;3(suppl):96–101.
2. Press OW, Eary JF, Appelbaum FR, et al. Radiolabeled-antibody therapy of B-cell lymphoma with autologous bone marrow support. *N Engl J Med.* 1993; 329:1219–1224.
3. Kaminski MS, Zasadny KR, Francis IR, et al. Radioimmunotherapy of B-cell lymphoma with [$^{131}$I]anti-B1 (anti-CD20) antibody. *N Engl J Med.* 1993;329: 459–465.
4. Wiseman GA, White CA, Stabin M, et al. Phase I/II $^{90}$Y-Zevalin (yttrium-90 ibritumomab tiuxetan, IDEC-Y2B8) radioimmunotherapy dosimetry results in relapsed or refractory non-Hodgkin's lymphoma. *Eur J Nucl Med.* 2000;27:766–777.
5. Richman CM, DeNardo SJ, O'Grady LF, DeNardo GL. Radioimmunotherapy for breast cancer using escalating fractionated doses of $^{131}$I-labeled chimeric L6 antibody with peripheral blood progenitor cell transfusions. *Cancer Res.* 1995; 55:5916s–5920s.
6. DeNardo SJ, Richman CM, Goldstein DS, et al. Yttrium-90/indium-111-DOTA-peptide-chimeric L6: pharmacokinetics, dosimetry and initial results in patients with incurable breast cancer. *Anticancer Res.* 1997;17:1735–1744.
7. Richman CM, Schuermann TC, Wun T, et al. Peripheral blood stem cell mobilization for hematopoietic support of radioimmunotherapy in patients with breast carcinoma. *Cancer.* 1997;80(supp):2728–2732.
8. Cagnoni PJ, Ceriani RL, Cole W, et al. Phase 1 study of high-dose radioimmunotherapy with Y-90-hu-Bre-3 followed by autologous stem cell support (ASCS) in patients with metastatic breast cancer [abstract]. *Cancer Biother Radiopharm.* 1998;13:328.
9. Wong JY, Somlo G, Odom-Maryon T, et al. Initial clinical experience evaluating yttrium-90-chimeric T84.66 anticarcinoembryonic antigen antibody and autologous hematopoietic stem cell support in patients with carcinoembryonic antigen-producing metastatic breast cancer. *Clin Cancer Res.* 1999;5(suppl):3224–3231.
10. Tempero M, Leichner P, Dalrymple G, et al. High-dose therapy with iodine-131-labeled monoclonal antibody CC49 in patients with gastrointestinal cancers: a phase I trial. *J Clin Oncol.* 1997;15:1518–1528.
11. Knox SJ, Goris ML, Trisler K, et al. Yttrium-90-labeled anti-CD20 monoclonal antibody therapy of recurrent B-cell lymphoma. *Clin Cancer Res.* 1996;2:457–470.
12. McEwan AJ, MacLean GD, Hooper HR, et al. MAb 170H.82: an evaluation of a novel panadenocarcinoma monoclonal antibody labelled with 99Tcm and with 111In. *Nucl Med Commun.* 1992;13:11–19.
13. Richman CM, DeNardo SJ, O'Donnell RT, et al. Dosimetry-based therapy in metastatic breast cancer patients using $^{90}$Y monoclonal antibody 170H.82 with autologous stem cell support and cyclosporin A. *Clin Cancer Res.* 1999;5(supp): 3243–3248.
14. Berger MJ. Distribution of absorbed dose around point sources of electrons and beta particles in water and other media. *J Nucl Med.* 1971;12(suppl):5–23.
15. Shen S, Duan J, Meredith RF, et al. Model prediction of treatment planning for dose-fractionated radioimmunotherapy. *Cancer.* 2002;94(suppl):1264–1269.
16. Coggle JE. Absence of late radiation effects on bone marrow stem cells. *Int J Radiat Biol Relat Stud Phys Chem Med.* 1980;38:589–595.
17. DeNardo GL, DeNardo SJ, Macey DJ, Mills SL. Quantitative pharmacokinetics of radiolabeled monoclonal antibodies for imaging and therapy in patients. In: Srivastava SC, ed. *Radiolabeled Monoclonal Antibodies for Imaging and Therapy*. New York, NY: Plenum; 1988:293–310.
18. Shen S, DeNardo GL, DeNardo SJ, Yuan A, DeNardo DA, Lamborn KR. Reproducibility of operator processing for radiation dosimetry. *Nucl Med Biol.* 1997;24:77–83.
19. Macey DJ, DeNardo SJ, DeNardo GL, DeNardo DA, Shen S. Estimation of radiation absorbed doses to the red marrow in radioimmunotherapy. *Clin Nucl Med.* 1995;20:117–125.
20. Lim SM, DeNardo GL, DeNardo DA, et al. Prediction of myelotoxicity using radiation doses to marrow from body, blood and marrow sources. *J Nucl Med.* 1997;38:1374–1378.
21. Shen S, Meredith RF, Duan J, et al. Improved prediction of myelotoxicity using a patient-specific imaging dose estimate for non-marrow targeting $^{90}$Y-antibody therapy. *J Nucl Med.* 2002;43:1245–1253.
22. Stabin MG. MIRDOSE: personal computer software for internal dose assessment in nuclear medicine. *J Nucl Med.* 1996;37:538–546.
23. Stabin MG, Eckerman KF, Bolch WE, Bouchet LG, Patton PW. Evolution and status of bone and marrow dose models. *Cancer Biother Radiopharm.* 2002;17: 427–433.
24. Bouchet LG, Bolch WE, Howell RW, Rao DV. S values for radionuclides localized within the skeleton. *J Nucl Med.* 2000;41:189–212.
25. Eckerman KF, Stabin MG. Electron absorbed fractions and dose conversion factors for marrow and bone by skeletal regions. *Health Phys.* 2000;78:199–214.
26. International Commission on Radiological Protection. Basic anatomical and physiological data for use in radiological protection: reference values: ICRP Publication 89. *Ann ICRP.* 2002;32:1–227.
27. van der Loo JC, Slieker WA, Kieboom D, Ploemacher RE. Identification of hematopoietic stem cell subsets on the basis of their primitiveness using antibody ER-MP12. *Blood.* 1995;85:952–962.
28. Carrasquillo JA, White JD, Paik CH, et al. Similarities and differences in $^{111}$In- and $^{90}$Y-labeled 1B4M-DTPA antiTac monoclonal antibody distribution. *J Nucl Med.* 1999;40:268–276.
29. DeNardo GL, Kroger LA, DeNardo SJ, et al. Comparative toxicity studies of yttrium-90 MX-DTPA and 2-IT-BAD conjugated monoclonal antibody (BrE-3). *Cancer.* 1994;73(suppl):1012–1022.

30. Akabani G, Poston JW Sr. Absorbed dose calculations to blood and blood vessels for internally deposited radionuclides. *J Nucl Med.* 1991;32:830–834.
31. Siegel JA, Wessels BW, Waston EE, et al. Bone marrow dosimetry and toxicity for radioimmunotherapy. *Antibody Immunoconj Radiopharm.* 1990; 3:213–233.
32. Sgouros G. Bone marrow dosimetry for radioimmunotherapy: theoretical considerations. *J Nucl Med.* 1993;34:689–694.
33. Breitz HB, Fisher DR, Wessels BW. Marrow toxicity and radiation absorbed dose estimates from rhenium-186-labeled monoclonal antibody. *J Nucl Med.* 1998;39: 1746–1751.
34. Shen S, DeNardo GL, Jones TD, Wilder RB, O'Donnell RT, DeNardo SJ. A preliminary cell kinetics model of thrombocytopenia after radioimmunotherapy. *J Nucl Med.* 1998;39:1223–1229.
35. Blumenthal RD, Lew W, Juweid M, Alisauskas R, Ying Z, Goldenberg DM. Plasma FLT3-L levels predict bone marrow recovery from myelosuppressive therapy. *Cancer.* 2000;88:333–343.
36. Bolch WE, Patton PW, Rajon DA, Shah AP, Jokisch DW, Inglis BA. Considerations of marrow cellularity in 3-dimensional dosimetric models of the trabecular skeleton. *J Nucl Med.* 2002;43:97–108.
37. Siegel JA, Yeldell D, Goldenberg DM, et al. Red marrow radiation dose adjustment using plasma FLT3-L cytokine levels: improved correlations between hematologic toxicity and bone marrow dose for radioimmunotherapy patients. *J Nucl Med.* 2003;44:67–76.
38. Deshpande SV, DeNardo SJ, Kukis DL, et al. Yttrium-90-labeled monoclonal antibody for therapy: labeling by a new macrocyclic bifunctional chelating agent. *J Nucl Med.* 1990;31:473–479.
39. O'Donnell RT, DeNardo SJ, Yuan A, et al. Radioimmunotherapy with $^{111}$In/$^{90}$Y-2IT-BAD-m170 for metastatic prostate cancer. *Clin Cancer Res.* 2001;7:1561–1568.
40. Shen S, DeNardo SJ, Richman CM, et al. Planning time for peripheral blood stem cell transfusion using patent-specific dosimetry for high dose radioimmunotherapy [abstract]. *J Nucl Med.* 2002;43(suppl):86P–87P.